Geochemical Journal, Vol. 40, pp. 523 to 535, 2006

Geochemistry of heavily altered Archean volcanic and volcaniclastic rocks of the Warrawoona Group, at Mt. Goldsworthy in the Pilbara Craton, Western Australia: Implications for alteration and origin

KENICHIRO SUGITANI,[1]* FUMIAKI YAMASHITA,[2] TSUTOMU NAGAOKA,[3] MASAYO MINAMI[4] and KOSHI YAMAMOTO[5]

[1]Department of Environmental Engineering and Architecture, Graduate School of Environmental Studies, Nagoya University, Nagoya 464-8601, Japan
[2]Department of Earth and Planetary Sciences, Graduate School of Science, Nagoya University, Nagoya 464-8603, Japan
[3]School of Informatics and Sciences, Nagoya University, Nagoya 464-8601, Japan
[4]Nagoya University Center for Chronological Research, Nagoya 464-8602, Japan
[5]Department of Earth and Environmental Sciences, Graduate School of Environmental Studies, Nagoya University, Nagoya 464-8601, Japan

(*Received November 9, 2005; Accepted May 19, 2006*)

The geochemical characteristics of Archean unusual siliceous rocks at Mt. Goldsworthy region in the Pilbara Craton were studied. The siliceous rocks have been assigned to the uppermost Warrawoona Group mafic volcanic rocks, and are overlain by quartz-rich sandstone units of the Strelley Pool Chert that probably represent continental margin sedimentation. The Warrwoona rocks have been heavily altered and are now composed dominantly of microcrystalline quartz, with subordinate mica, Fe-Ti oxides and unidentified silicates; original magmatic textures are only locally preserved. The complex alteration is assumed to result from multiple events including weathering during subaerial exposure, circulation of hydrothermal fluids, and metasomatic silicification. During alteration, Al, Ti, Zr, Th, Cr and Sc remained immobile, although their concentrations were lowered by a substantial increase in silica. Mutual ratios of these immobile elements such as Al_2O_3/TiO_2 Cr/Th, Th/Sc, Cr/Al_2O_3 and Zr/TiO_2 and comparison with the least-altered contemporaneous mafic-ultramafic rocks in the Pilbara Craton show that the altered rocks originated from high-MgO rocks such as komatiite and high-MgO basalt, possibly of Al-depleted type. The Mt. Goldsworthy rocks have significantly higher Th/Sc (0.024–0.1) values compared with primitive mantle values (0.005) and komatiite (0.01). This feature is interpreted as a result of crustal contamination, which is consistent with the early evolution of continental crust.

Keywords: Archean, Pilbara, altered mafic-ultramafic rocks, origin, geochemistry

INTRODUCTION

In this study, we discuss the origin of heavily altered Archean rocks distributed at southern margin of the Mt. Goldsworthy region in the northeastern Pilbara Craton, based on whole-rock major and trace element data including rare-earth elements, Zr, Th, Sc and Hf, and microanalyses of some constituent minerals. The rocks occur as a narrow basal unit that is assigned to the Warrawoona Group mafic volcanic rocks (Smithies, 2002) and are overlain with siliciclastic metasedimentary rocks that record an Archean shallow to subaerial sedimentary environment (Sugitani *et al*., 2003). The sedimentary succession has recently been assigned to the Strelley Pool Chert that represents Earth's oldest continental margin sequence (Van Kranendonk *et al*., 2002). Thus the Warrawoona mafic rocks just below the Strelley Pool Chert at Mt. Goldsworthy are of special interest, in the context of early evolution of continental crust. Evolution of continental crust during the early Precambrian time has long been a major issue in the earth sciences (e.g., Taylor and McLennan, 1985; Condie, 1993; Gao and Wedepohl, 1995; Smithies *et al*., 2003; Smithies and Van Kranendonk, 2005). The early (>3.0 Ga) evolution of continental crust within the Pilbara Craton has been claimed, based on the record of erosion of ~3.5 Ga granitoid basement (Buick *et al*., 1995) and U-Pb zircon ages (McNaughton *et al*., 1993; Smithies *et al*., 1999; Thorpe *et al*., 1992). Trace element and isotopic signatures of the Warrawoona mafic to ultramafic volcanic rocks suggest the contamination of crustal materials (Green *et al*., 2000). In such circumstances, new data from Mt. Goldsworthy would potentially provide further evidence for early evolution of continental crust and related magmatic processes.

*Corresponding author (e-mail: sugi@info.human.nagoya-u.ac.jp)

Chemical compositions of Archean greenstones have in most cases been modified to various degrees by metamorphism, alteration and weathering (e.g., Arndt *et al*., 1989; Arndt, 1994; Condie *et al*., 1977; Condie, 1981; Green *et al*., 2000; Gruau *et al*., 1992; Polat *et al*., 2002; Smith *et al*., 1980, 1984; Sun and Nesbitt, 1978; Tourpin *et al*., 1991; Van Kranendonk and Pirajno, 2004). In the case of the Mt. Goldsworthy rocks, their alteration was intense and they are now unusually siliceous rocks whose SiO_2 concentration is up to 90%; their original rock types have been inferred only from relict texture and Cr-Zr-Al-Ti systematics (Sugitani *et al*., 2003). Such heavily altered greenstones have generally been ruled out from most of previous geochemical studies that were aimed at crustal evolution and magma genesis. However, in situations in which unaltered and relatively fresh samples are not available as is the situation at Mt. Goldsworthy, we cannot avoid studying heavily altered rocks. In this study we focus on high field strength and rare-earth elements (Zr, Th, Ti and REE), since these elements are generally resistant to post-magmatic events and are expected to provide important information about the origins and tectonic environments of altered Archean greenstones (e.g., Jochum *et al*., 1991; McCuaig *et al*., 1994; Polat *et al*., 1999; Xie *et al*., 1993).

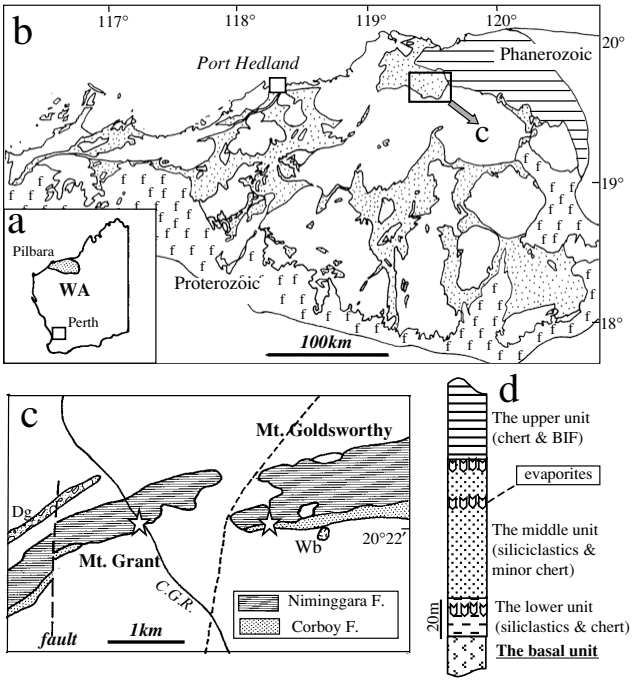

Fig. 1. Geological map of the studied area. a: Map of Western Australia. b: The overview of the Pilbara Craton. The dotted are is greenstones (after Van Kranendonk et al., 2002). c: The local geological map of Mt. Goldsworthy and Mt. Grant (after Smithies, 2002). The stars show sampling locations. C.G.R. shows Coongan Goldsworhty Road. Dg: De Grey Groups, Wb: Warrawoona Group. Geological interpretation (see Legend) of this area is after Smithies (2002), and is revised recently (see text). d: Representative stratigraphy of Mt. Goldsworthy volcanic-sedimentary succsession (after Sugitani et al., 2003).

GEOLOGIC BACKGROUND AND SAMPLING

According to the recent lithostratigraphic scheme for Archean granite-greenstone belts (Van Kranendonk *et al*., 2004), the Pilbara Supergroup in the eastern Pilbara Craton comprises four groups, namely the Warrawoona, the Kelly, the Sulfur Springs and the Gorge Creek Groups, in ascending stratigraphic order. Smithies (2002) interpreted the volcanic rocks at the southern margin of Mt. Goldsworthy and Mt. Grant as belonging to the Warrawoona Group, although not to any specific members. The 3.52–3.43 Ga Warrawoona Group is defined as comprising four subgroups—the Coonterunah, Talga Talga, Coongan, and Salgash Subgroups (Van Kranendonk *et al*., 2004). The group consists mainly of mafic-ultramafic igneous rocks (tholeiitic basalt and gabbro, high-Mg basalt, peridotitic komatiite, and high-Al basalt) with intercalated intermediate to felsic volcanic rocks and sedimentary rocks (chert and volcaniclastics; Hickman, 1983; Glikson and Hickman, 1981). The tectonic setting of eruption and the magmatic process producing the mafic to ultramafic rocks are controversial; for example, Barley (1993) concluded that the Warrawoona mafic-ultramafic volcanic rocks were formed in volcanic arc and near-arc settings, whereas Green *et al*. (2000) claimed that the rocks were erupted onto continental basement.

The Warrawoona volcanic rocks at the Mt. Goldsworthy are overlain by a sedimentary succession as noted earlier, which is correlated to the Strelley Pool Chert of the Kelly Group. The Strelley Pool Chert was first described in the Pilgangoora Belt, where it comprises a basal, quartz-rich sandstone with minor conglomerate, silicified laminated carbonates, mafic volcaniclastics, and locally pseudomorphic evaporitic minerals (Lowe, 1980, 1983). Similarly, the Mt. Goldsworthy sedimentary succession is composed predominantly of quartz-rich sandstones with minor conglomerate and evaporitic layers in its lower and middle portions (Fig. 1). The evaporitic layers contain giant vertically or sub-vertically oriented pseudo-hexagonal crystal pseudomorphs, which were interpreted as nahcolite ($NaHCO_3$) by Sugitani *et al*. (2003). The Strelley Pool Chert that represents Earth's oldest continental margin sequence is now correlated over a distance of 220 km across most of the East Pilbara granite-greenstone terrane (Van Kranendonk *et al*., 2002). The sedimentary sequence was deposited on a regional unconformity above the Warrawoona Group and is overlain conformably by the Euro Basalt that consists of

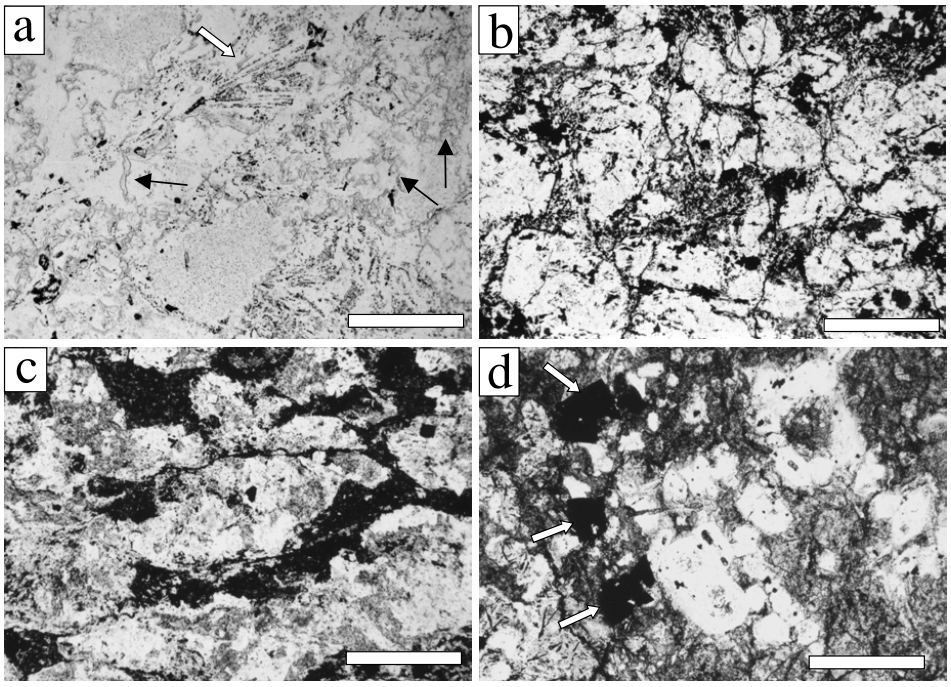

Fig. 2. Photomicrographs of altered rocks. Plane polarized light. Scale bars are 500 μm. a) Fuchsite-rich sample (GW98-1-1). The arrows show fuchsite (slightly gray mineral with high refractive index in the photo). The white arrow shows the relict of prismatic minerals now outlined by Ti-oxide particles. b) Cumulate-like texture (GW98-1-4). Lath- to hexagonal-shaped pseudomorphs are closely packed. c) Nodule-like texture (GW98-1-5). Interstices are yellowish brown, possibly enriched in iron oxides. d) Chlorite-rich, less silicified sample (VMGG2). The white arrows show oxidized iron-bearing carbonate rhombs. Chlorite is ubiquitous (gray). White lath- to hexagonal-shaped silicified crystals can also be seen.

<1.5 km thick basal komatiitic rocks and overlying ~5 km thick basaltic rocks (Van Kranendonk *et al.*, 2002, 2004). The volcanism of the Euro Basalt from 3.35 to 3.32 Ga is interpreted to have occurred as continental flooding (Van Kranendonk and Pirajno, 2004 and references therein).

The majority of samples analyzed for this study were collected from the southwestern margin of Mt. Goldsworthy (15 samples), with additional samples from the stratigraphically correlative portion at Mt. Grant, 2 km west of Mt. Goldsworthy (2 samples; Fig. 1). At the Mt. Goldsworthy site, highly silicified, light gray to green, bright green and brownish yellow basal rocks occur. White, irregularly shaped quartz bodies of up to 1 m in length are found locally although cross cutting chert dykes are scarcely developed. The color of rocks at the outcrop is various, at least partially due to surface weathering. Near the top of this unit, light green, light gray and black cherts occur locally as small (<1 m-long) lenses or massive blocks of irregular shape. The relationship with the overlying siliciclastic unit (the Strelley Pool Chert) is not always clear; however, local erosional contact is implied from abundant mafic to ultramafic clasts in the lowermost sandtones. At the Mt. Grant site, the basal massive rocks are less silicified and dark green, with reddish brown patches. In both Mt. Goldsworthy and Mt. Grant, no indicative structures such as pillow, layering and cumulative structures are observed.

PETROGRAPHY

Mt. Goldsworthy samples

The basal rocks at Mt. Goldsworthy are composed predominantly of quartz, with subordinate Fe-oxides, Ti-oxides and mica, and traces of carbonates and sulfides. The quartz grains are mostly microcrystalline (less than 10 μm in length) and locally mixed with larger grains (up to 500 μm). Fe-oxides and Ti-oxides occur as granules or flakes, and are often closely associated with each other. Micas are white, light bluish green, or brownish-yellow, and occur as masses or lamina-like aggregations, or as scattered flakes (Fig. 2a). Minute carbonate particles are occasionally found within relatively large quartz grains. Sulfide occurs mostly as relatively small (<10 μm) euhedral grains.

In spite of their relatively simple mineral assemblage described above, the Mt. Goldsworthy samples are characterized by a variety of textures. Some samples contain

Table 1. Chemical compositions of the basal rocks from Mt. Goldsworthy (GW) and Mt. Grant (VMGG)

Mt. Grant																	
Sample No.	GW98-1-1	GW98-1-2	GW98-1-3	GW98-1-4	GW98-1-5	GW98-1-6	GW98-1-7	GW98-1-9	GW98-1-10	GW98-1-11	GW98-1-12	GW95-1-1	GW99-0-3	GW99-2-2	GW99-0-1	VMGG1	VMGG2
Petrography	Igneous	Unclear	Unclear	Igneous	Clastic	Igneous	Igneous	Unclear	Clastic	Igneous	Unclear	Unclear	Unclear	Unclear	Unclear	Igneous	Igneous
SiO_2 (wt%)	86.72	75.63	70.2	86.46	88.33	88.98	82.99	88.12	92.48	95.7	86.21	92.52	89.74	95.46	93.69	65.39	64.76
TiO_2	0.79	0.99	0.68	1.06	0.64	0.93	0.96	1.06	0.6	0.43	1.21	0.45	0.67	0.24	0.43	1.49	1.74
Al_2O_3	4.32	6.55	4.67	5.52	3.53	4.75	5.79	5.69	3.58	2.98	5.52	2.53	4.44	1.41	2.3	8.67	8.86
Fe_2O_3(total)	4.98	11.72	18.67	3.23	4.41	3.14	6.72	1.79	0.59	0.23	3.08	0.8	0.34	0.05	0.33	18.94	18.69
MnO	<0.001	<0.001	<0.001	<0.001	<0.001	<0.001	0.25	0.004	<0.001	<0.001	<0.001	<0.001	<0.001	<0.001	<0.001	0.05	0.061
MgO	0.09	0.05	0.03	0.17	0.08	0.11	0.11	0.56	0.07	0.08	0.32	0.07	0.08	0.03	0.10	3.51	4.03
CaO	0.22	0.05	0.07	0.05	0.08	0.07	0.09	0.08	0.04	0.03	0.02	0.02	0.02	0.02	0.02	0.13	0.08
Na_2O	0.11	0.03	0.21	0.17	0.04	0.02	0.10	0.09	0.08	0.09	0.05	<0.01	0.08	0.15	<0.01	0.13	0.09
K_2O	0.04	0.04	0.05	0.04	0.03	0.03	0.05	0.05	1.16	0.89	1.38	0.73	1.08	0.45	0.75	0.04	0.04
P_2O_5	0.075	0.072	0.15	0.02	0.051	0.08	0.035	0.014	0.012	0.008	0.095	0.018	0.019	0.01	0.011	0.25	0.15
H_2O(total)	2.3	4.06	4.17	2.28	1.88	2.08	2.93	2.66	0.55	0.49	1.52	0.67	0.97	0.23	0.4	5.11	5.07
C(total)	0.05	0.03	0.03	0.01	0.02	0.01	0.01	0.04	0.01	0.01	0.01	0.03	0.02	0.01	0.01	0.02	0.01
S(total)	<0.01	<0.01	<0.01	<0.01	<0.01	<0.01	<0.01	<0.01	<0.01	<0.01	<0.01	<0.01	0.01	<0.01	<0.01	<0.01	<0.01
Total	99.7	99.22	98.93	99.01	99.09	100.2	100.04	100.16	99.17	100.94	99.42	97.84	97.47	98.06	98.04	103.73	103.58
Co (ppm)	5	2	14	9	7	14	29	8	5	6	6	3	6	5	7	126	70
Ni	59	121	154	46	50	87	47	59	19	15	73	17	21	12	19	547	439
Cu	101	76	117	26	71	124	55	34	24	14	89	14	19	7	11	n.a.	n.a.
Zn	31	56	98	17	19	24	35	12	21	46	21	13	31	7	19	83	24
Rb	<1	<1	<1	<1	<1	<1	<1	<1	31	27	58	20	35	15	29	n.a.	n.a.
Sr	7	<1	2	17	5	53	37	22	1	1	1	<1	4	6	<1	n.a.	n.a.
Y	9	12	12	9	11	16	11	11	13	8	13	10	10	6	13	n.a.	n.a.
Zr	65	91	67	88	60	70	86	77	60	35	88	38	57	18	40	155	154
Pb	7	5	1	5	5	1	<1	3	3	1	3	6	6	3	3	n.a.	n.a.
Ba	114	87	196	236	197	166	871	392	147	166.4	137.6	112	226	104.1	70	n.a.	n.a.
Cr	1845	904	1501	1293	1443	1325	818	1999	1146	1510	2317	686	1146	718	678	2002	1392
Th	0.66	0.95	0.81	0.82	0.44	0.57	1.23	0.81	0.51	—	0.99	0.52	0.7	—	0.32	1.22	1.21
Sc	17.7	30.6	28.9	16.7	18.4	13.5	16.2	25	12.3	12.7	35.9	5.2	11.4	6.2	8.3	40.4	41.1
Hf	—	—	—	1.6	—	1.6	1.8	1.5	1.4	—	1.7	—	1.1	—	—	2.2	2.2
As	—	—	10.9	—	1.3	—	—	—	103.2	39.8	72.9	83.4	39.1	12	4.1	91.4	—
Sb	3.7	—	—	2.2	—	—	—	4.5	44.6	3.6	3.9	13.3	3.7	—	2.4	2.6	—
Method	INAA	INAA	INAA	INAA	ICP-MS	ICP-MS	ICP-MS	INAA	INAA	INAA	INAA	ICP-MS	INAA	INAA	ICP-MS	INAA	INAA
La	2.49	5.05	3.48	7.24	1.125	17.32	6.311	5.76	3.989	4.481	6.976	5.475	5.171	7.299	4.28	11.8	11.8
Ce	—	—	—	—	3.016	35.486	25.628	—	—	—	—	10.485	—	—	9.062	34.6	31
Pr	n.a.	n.a.	n.a.	n.a.	0.457	4.509	1.916	n.a.	n.a.	n.a.	n.a.	1.327	n.a.	n.a.	1.283	n.a.	n.a.
Nd	n.a.	n.a.	n.a.	n.a.	2.337	19.304	8.225	n.a.	n.a.	n.a.	n.a.	5.64	n.a.	n.a.	5.878	n.a.	n.a.
Sm	1.27	2.23	1.73	1.62	0.829	4.188	2.058	1.085	1.67	1.335	2.291	1.296	1.62	1.346	1.502	5.8	4.49
Eu	n.a.	n.a.	0.58	n.a.	0.346	1.129	0.607	—	—	n.a.	n.a.	0.381	0.51	—	0.499	1.83	1.38
Gd	n.a.	n.a.	n.a.	n.a.	1.265	4.249	2.036	n.a.	n.a.	n.a.	n.a.	1.336	n.a.	n.a.	1.675	n.a.	n.a.
Tb	n.a.	n.a.	n.a.	n.a.	0.24	0.542	0.313	—	n.a.	n.a.	n.a.	0.198	—	—	0.268	—	—
Dy	n.a.	n.a.	n.a.	n.a.	1.602	2.844	1.879	n.a.	n.a.	n.a.	n.a.	1.192	n.a.	n.a.	1.682	n.a.	n.a.
Ho	n.a.	n.a.	n.a.	n.a.	0.328	0.491	0.355	n.a.	n.a.	n.a.	n.a.	0.24	n.a.	n.a.	0.34	n.a.	n.a.
Er	n.a.	n.a.	n.a.	n.a.	0.933	1.193	0.998	n.a.	n.a.	n.a.	n.a.	0.687	n.a.	n.a.	0.96	n.a.	n.a.
Tm	n.a.	n.a.	n.a.	n.a.	0.133	0.151	0.149	n.a.	n.a.	n.a.	n.a.	0.095	n.a.	n.a.	0.133	n.a.	n.a.
Yb	0.98	1.08	1.03	0.89	0.861	0.898	0.996	0.909	0.931	—	1.047	0.604	1.023	0.311	0.848	2.28	1.7
Lu	0.16	0.24	0.19	—	0.122	0.125	0.141	—	0.16	—	—	0.093	0.13	—	0.123	0.33	0.22
Y	n.a.	n.a.	n.a.	n.a.	7.749	11.22	7.231	n.a.	n.a.	n.a.	n.a.	6.509	n.a.	n.a.	8.836	n.a.	n.a.
Al_2O_3/TiO_2	5.5	6.6	6.9	5.2	5.5	5.1	6	5.4	6	7	4.6	5.2	6.7	6	5.4	5.8	5.1
Zr/TiO_2	82.3	91.9	98.5	83	93.8	75.3	89.6	72.6	100	81.4	72.7	84.4	85.1	75	93	104	88.5
Cr/Th	2795	952	1853	1577	3280	2325	665	2468	2247	—	2340	1319	1637	—	2119	1641	1150
Cr/Zr	28.4	9.9	22.4	14.7	24.1	18.9	9.5	26	19.1	43.1	26.3	18.1	20.1	39.9	17	12.9	9
Th/Sc	0.037	0.031	0.028	0.049	0.024	0.042	0.076	0.032	0.041	—	0.028	0.1	0.061	—	0.039	0.03	0.029
La/Sc	0.14	0.17	0.12	0.43	0.06	1.28	0.39	0.23	0.32	0.35	0.19	1.05	0.45	1.18	0.52	0.29	0.29

Table 2. Results of EPMA analyses of mica and other aluminosilicates

	Point-1	Point-2	Point-3	Point-4	Point-5	Point-6	Point-7	Point-8	Point-9
GW98-1-2									
SiO_2 (wt%)	43.71	34.21	16.14	29.93	16.94	10.42	67.3	44.36	54.2
TiO_2	0.13	0.07	0.08	0.09	0.09	0.09	0.06	0.04	0.03
Al_2O_3	12.06	13.95	17.54	26.96	17.03	12.07	8.45	15.89	24.75
FeO	34.35	34.18	47.86	28.25	44.17	53.01	18.65	15.73	8.37
MgO	0.03	0.02	0.02	0.01	0.04	0.04	0.02	0.03	0.05
Na_2O	0.02	0.05	0.03	0.03	0.05	0.01	0.01	0.03	0.02
K_2O	0.02	0.03	0.02	0.02	0.03	n.d.	0.02	0.03	0.04
BaO	n.d.	n.d.	n.d.	n.d.	0.04	n.d.	0.03	n.d.	0.08
Cr_2O_3	0.28	0.24	0.4	0.55	0.45	0.25	0.18	0.29	0.33
Total	90.58	82.74	82.08	85.84	78.84	75.89	94.71	76.4	87.86
GW98-1-11									
SiO_2 (wt%)	47.66	45.93	47.11	46.44	94.72	46.94	49.19	47.56	47.59
Al_2O_3	33.81	32.89	33.93	32.33	2.77	33.53	33.76	33.28	33.58
FeO	0.22	0.26	0.2	0.24	0.03	0.25	0.18	0.25	0.22
MgO	0.6	0.52	0.53	0.65	0.07	0.56	0.74	0.68	0.67
Na_2O	0.4	0.44	0.52	0.29	0.02	0.36	0.33	0.37	0.32
K_2O	10.2	9.95	10.04	10.24	0.98	10.22	9.75	10.15	10.3
BaO	0.05	0.06	0.03	0.08	n.d.	0.08	0.03	0.14	0.12
Cr_2O_3	3.22	2.87	3.1	2.64	0.22	2.97	2.74	3.01	3.13
Total	96.17	92.91	95.46	92.92	98.83	94.91	96.73	95.45	95.93
VMGG2									
SiO_2 (wt%)	24.75	24.68	24.33	23.84	23.88	29.11	25.78	25.2	28.59
TiO_2	0.05	0.03	0.02	0.03	0.01	0.07	0.02	0.07	0.05
Al_2O_3	21.72	21.36	21.37	20.95	21.15	21.52	20.93	21.41	25.94
FeO	31.47	30.54	31.1	31.39	31.77	26.53	29.04	29.87	25.16
MgO	10.14	10.07	10.01	9.72	9.87	6.59	9.23	9.67	7.41
Na_2O	n.d.	n.d.	0.03	n.d.	0.01	0.03	0.06	n.d.	n.d.
K_2O	0.02	n.d.	n.d.	n.d.	n.d.	0.41	0.16	0.06	0.01
BaO	0.03	0.06	0.06	0.06	0.04	0.06	0.02	n.d.	0.03
Cr_2O_3	0.71	0.63	0.67	0.65	0.64	0.84	0.88	0.99	0.25
Total	88.87	87.38	87.61	86.65	87.37	85.16	86.1	87.27	87.44

prismatic, lath-shaped and pseudo-hexagonal crystal pseudomorphs of polycrystalline quartz up to 2 mm in length (Fig. 2b), which are interlocked or closely packed with each other. They are in many cases outlined with slightly yellowish minute particles, which are assumed to be Ti-oxides. Skeletal rhomb- to hopper-shaped crystal pseudomorphs composed of Fe- and Ti-oxides (rutile and anatase) are also present. The pseudo-hexagonal, rhombic and skeletal habits of the pseudomorphs resemble pyroxene and olivine phenocrysts in mafic to ultramafic volcanic rocks (e.g., Nisbet *et al*., 1993; Orpen *et al*., 1993). They are dispersed in a quartz-rich matrix. Closely packed lath-shaped pseudomorphs now composed of polycrystalline quartz resemble a cumulate texture (Figs. 2b and d for Mt. Grant sample; e.g., Arndt, 1994; Duchač and Hanor, 1987; Orpen *et al*., 1993). Interstices of these packed pseudomorphic grains are composed of brownish-yellow oxides that are probably mixture of Fe- and Ti-oxides. In addition to these crystallographic textures (see also figure 4 of Sugitani *et al*., 2003), a nodular texture is observed in one sample from Mt. Goldsworthy (Fig. 2c). Irregularly shaped nodule-like bodies are composed of polycrystalline quartz containing abundant minute oxide particles. The "nodules" contain rhomb- to cubic-shaped crystal ghosts. The matrix is enriched in oxides, although in some portions the relationship between nodules and matrix is transitional. Also some light grayish green rocks characterized by abundant lath-shaped pseudomorphs contain angular grains composed of microcrystalline quartz. The grains are more likely detrital, rather than crystallized. The rest of the samples do not show either magmatic or clastic textures.

Mt. Grant samples

The Mt. Grant samples are characterized by a lower abundance of quartz and by enrichment of chlorite compared with those from Mt. Goldsworthy. Pseudomorphic minerals replaced by quartz are common. Particles of Fe- and Ti-oxides are also abundant in the rocks, and locally display textures of an anastomosing network. Rhombic

crystals composed of Fe-oxides are common (Fig. 2d). The crystals tend to be more abundant in and around winding narrow quartz veins less than 5 mm wide. These veins are enriched in impurities such as oxides and silicates and do not always have sharp contact with the matrix. Dendritic and hopper crystal skeletons composed of Fe- and Ti-oxides, similar to those in Mt. Goldsworthy samples, are also present. Locally, lath- to pseudo-hexagonal-shaped pseudomorphs are closely packed, like some of Mt. Goldsworthy samples.

Analytical Methods

Major elements were analyzed by an automatic X-ray fluorescence spectrometer (XRF) using fusion glasses made from a mixture of powdered sample and flux ($Li_2B_4O_7$) in the proportion of 1:5 (Sugisaki *et al*., 1977). The total concentrations of C, H and S were determined using an elemental analyzer. The analyses of the minor elements (including rare-earth elements) were performed using XRF, a graphite-furnace atomic adsorption spectrometer (GFAA), an inductively coupled plasma mass spectrometer (ICP-MS) and instrumental neutron activation analysis (INAA).

Cobalt, Ni, Cu, Zn, Pb, Rb, Sr, Zr and Ba were analyzed by XRF; pressed discs containing a mixture of powdered sample and binder in the proportion of 2:3 were used, following the method of Sugitani and Mimura (1998). Chromium, Th, Sc, Hf, Sm, Eu, Yb, and Lu in all samples were measured by INAA following the method of Shibata *et al*., (2001). All rare-earth elements (REEs), and Y of selected samples were analyzed by ICP-MS. The preparation of sample solution for the REEs and Y for ICP-MS analyses was conducted as follows: 200~500 mg samples were decomposed twice by 9 ml HF/$HClO_4$ acid (2:1 in v/v ratio) at 160°C, and subsequently evaporated to dryness. The residues were dissolved in about 2 ml of 1.7N-HCl and centrifuged at 12000 rpm for 10 min. The sample solutions were separated from the major elements using an AG50W-X8 cation exchange column. The solutions including REEs were evaporated to dryness and dissolved in about 15 g of 2%-nitric acid. This solution was subjected to ICP-MS analysis using 157 ppb In and Bi as internal standards. The analytical errors of the REEs estimated by determination of JB-1a, published by Geological Survey of Japan, were about 1–3%. The analytical results are listed in Table 1. Data of REE obtained by ICP-MS and those by INAA are nearly identical with each other, within 5% for La and Sm, and 10% for Yb and Lu.

In addition, some constituent minerals such as mica and other alumino-silicates were analyzed using an electron microprobe analyzer (EPMA), following the method of Enami *et al*. (2004). The analytical results are listed in Table 2.

Results

Major elements of whole rock samples

The concentrations of the major elements of the Mt. Goldsworthy samples indicate that the chemical compositions of the Mt. Goldsworthy rocks are quite different from those of any other volcanic rocks (Table 1). The Mt. Goldsworthy rocks have high SiO_2 concentrations (>80% for all but two samples), and the concentrations of TiO_2 and Al_2O_3 range from 0.24 to 1.21% and from 1.41 to 6.55%, respectively. The Al_2O_3/TiO_2 values range from 4.6 to 7.0. The concentration of Fe_2O_3 (total Fe as Fe_2O_3) and P_2O_5 vary widely from 0.05 to 18.6% and from 0.01 to 0.15%, respectively. Most samples are very low in MnO, MgO, CaO, and Na_2O concentrations (<0.2%). The samples may be classified into two groups based on K_2O concentration: the K_2O concentrations of half the samples are less than 0.05%, whereas the others exceed 0.4% (and are as high as 1.38%). The high-K samples tend to be poor in Fe (0.05~3.08% as Fe_2O_3) in comparison with the low-K samples (1.79~18.67% as Fe_2O_3).

Compared with the Mt. Goldsworthy samples, the Mt. Grant basal rocks exhibit lower SiO_2 (<70%) and higher TiO_2, Al_2O_3, Fe_2O_3, MgO, P_2O_5, and H_2O concentrations. The Al_2O_3/TiO_2 values (5.8 and 5.1) are within the range of the Mt. Goldsworthy samples (4.6–7.0). The samples are characterized by very low concentrations of K_2O (<0.05%), and high Fe_2O_3 (>18%).

Minor elements of whole rock samples

The Co, Ni, Cu, Zn, Pb, Sr, Ba, and Rb contents of the Mt. Goldsworthy samples are highly variable from sample to sample. Cobalt, Ni, Cu, Zn and Pb concentrations range from 2 to 29 ppm, from 12 to 154 ppm, from 7 to 124 ppm, from 7 to 98 ppm, and from <1 to 7 ppm, respectively. Sr and Ba concentrations also differ greatly, from <1 to 53 ppm and from 70 to 871 ppm, respectively. Rb was detected (15~58 ppm) in only half of the samples showing high K_2O concentrations.

The Zr, Cr, Th, Sc and Hf contents are less variable and vary within an order of magnitude. The samples commonly have very high Cr concentrations (680~2300 ppm). Scandium concentration varies from 5.2 to 36 ppm. Zirconium, Th and Hf concentrations range from 18 to 88 ppm, from 0.32 to 1.23 ppm, and from 1.1 to 1.8 ppm, respectively. Among the REEs (La, Sm, Yb and Lu), the La concentration varies the most widely from 1.1 to 17.3 ppm, which contrasts markedly with the relatively narrow concentration range of Yb (0.3–1.1 ppm). The chondrite-normalized REE patterns of the five samples analyzed by ICP-MS are shown in Fig. 3. These examples tend to display similar patterns consisting of a smooth decrease from LREE to HREE, with the exception of one sample, which exhibits a nearly flat pattern. One sample

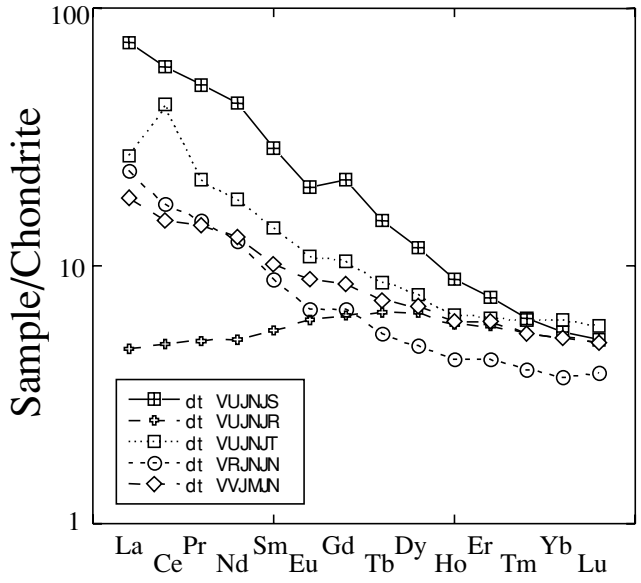

Fig. 3. Chondrite (C1) (Anders and Grevesse, 1989)-normalized REE patterns for the Mt. Goldsworthy altered rocks.

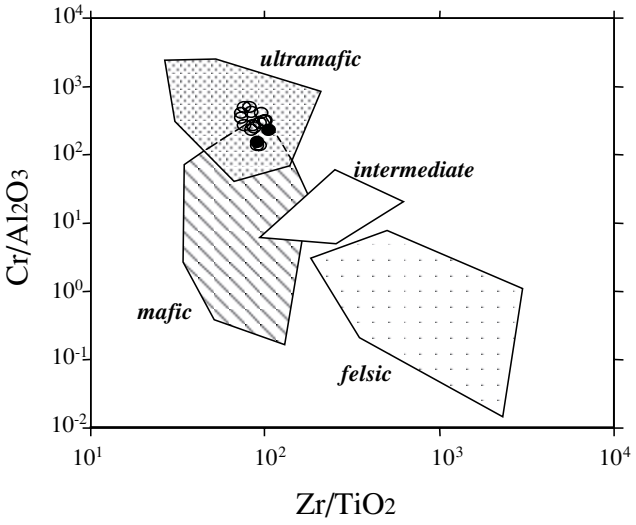

Fig. 4. Distribution of the altered rocks from Mt. Goldsworthy (open circles) and Mt. Grant (closed ones) on the discrimination diagram (Zr/TiO_2 and Cr/Al_2O_3) for Archean altered felsic-intermediate-mafic-ultramafic rocks (Sugitani, 2000).

shows a distinct positive Ce-anomaly. The La/Yb ratios in all samples analyzed are from 1.3 to 23.5 (Table 1).

In common with the major elements excluding Si, the minor elements of the Mt. Grant samples tend to be present in higher concentrations than the Mt. Goldsworthy samples. However, the relative ratios of the high field strength elements (Zr, Th, Sc, Ti and REE), Cr, and Al are mostly within the corresponding ranges for Mt. Goldsworthy (Table 1).

Chemical composition of selected minerals

We analyzed 1) a yellowish-brown mixture of oxides in a relatively Fe-enriched sample (GW98-1-2; equivalent to the black portion in Fig. 2b), 2) a bluish-green mica in a K-rich sample (GW98-1-11; Fig. 2a), and 3) a dark green mineral in a less-altered sample (VMGG2; Fig. 2d). Their chemical compositions are listed in Table 2 and some interpretations are presented below.

1) The analytical results obtained for the yellowish-brown material show that they contain wide variations in SiO_2, Al_2O_3 and FeO concentrations. Though rather variable, significantly high Cr_2O_3 contents are also observed, whereas the MgO, Na_2O and K_2O contents are quite low. The material appear to be not composed of any specific mineral, but rather of a mixture of alumino-silicates and Fe-oxides.

2) The bluish-green mica mineral is characterized by high K_2O and Cr_2O_3 concentrations and thus identified as fuchsite. It contains trace amounts of Na_2O and MgO. The high-K samples in addition to GW98-1-11 contain bright green to light blue patches and veins visible in hand specimens, which are thus probably fuchsite also.

3) The dark green mineral is optically identifiable as a chlorite group mineral, an observation supported by its chemical composition being characterized by high concentrations of MgO. It may also be noted that the mineral is characterized by relatively high Cr_2O_3 contents.

DISCUSSION

Recognition of immobile elements

As mentioned earlier, chemical compositions of Archean rocks have in most cases been modified to various degrees by metamorphism, alteration and weathering. This is also the case for the Mt. Goldsworthy rocks. The bulk chemical compositions of the rocks indicate that they are unusually siliceous for igneous rocks. Additionally, the presence of ubiquitous pseudomorphic minerals now composed of micro to granular quartz is diagnostic for silicification. In addition to silicification, other alteration events related to the formation of carbonate (carbonatization), chlorite (chloritization) and fuchsite (K-metasomatism) are inferred on petrographic and chemical grounds to have taken place, as discussed in detail in the later section.

In order to study the origin of heavily altered rocks like these, immobile elements represented by Zr and Ti could be a strong tool (Condie and Wronkiewicz, 1990; Cullers *et al*., 1993; Duchač and Hanor, 1987; Lowe, 1999), although it may be cautioned that under certain peculiar alteration conditions, even Zr and Ti can be mobilized (e.g., Salvi and Williams-Jones, 1996). Concern-

Table 3. Correlation coeffifients between HFSEs, Cr, Al, and SiO_2

	TiO_2	Al_2O_3	Zr	Cr	Th	Sc	SiO_2	La	Sm	Yb
TiO_2	1	0.96	0.96	0.53	0.83	0.86	–0.77	0.53	0.73	0.81
Al_2O_3		1	0.97	0.46	0.89	0.87	–0.85	0.46	0.74	0.87
Zr			1	0.45	0.84	0.86	–0.86	0.49	0.79	0.92
Cr				1	0.33	0.64	–0.31	0.10	0.26	0.49
Th					1	0.76	–0.76	0.38	0.58	0.70
Sc						1	–0.86	0.28	0.62	0.79
SiO_2							1	–0.32	–0.69	–0.83
La								1	0.82	0.40
Sm									1	0.82
Yb										1

Table 4. Th/Sc, Cr/Th and Cr/Zr for Archean Igneous series and Mt. Goldsworthy rocks

	Granite	Tonalite	Felsic V.	Andesite	Basalt	Komatiite	Mt. Goldsworthy
Th/Sc	10	1.3	0.13	0.15	0.02	0.0035	0.02~0.1
Cr/Th	0.2	6.5	12.5	67	500	>10000	1300~4800
Cr/Zr	0.04	0.3	0.12	1.4	5.5	>75	14~51

Note: Data for average values of igneous rocks are quoted from Condie and Wronkiewicz (1990) and Condie (1993).

ing the Mt. Goldsworthy altered rocks, the elements such as Zr, Ti, Sc, Th and Al are indeed immobile, because they correlate positively with one another ($r > 0.75$) (Table 3). Their inverse correlation with SiO_2 ($r = –0.75$), on the other hand, suggests silica addition during alteration. However, this silica addition was not accompanied by substantial remobilization of these 5 "immobile elements". Consequently, their mutual ratios could be used as a discriminator when studying the origin of the Mt. Goldsworthy rocks.

Compared with these 5 "immobile" elements showing high mutual correlation coefficients, Cr and REEs need more careful consideration. The lower correlation coefficient of Cr with other "immobile" elements suggests its redistribution during alteration events. Among the three rare-earth elements in Table 3, Yb tends to show the highest positive correlation with elements such as Zr, Ti and Al, whereas La exhibits the lowest. The behavior of Cr, La, Sm, and Yb during alteration will be discussed in the later section.

Origins of the Mt. Goldsworthy basal altered rocks

Sugitani *et al.* (2003) suggested that the basal rocks at Mt. Goldsworthy were originally of mafic to ultramafic composition, based on the distribution patterns discernible in a Zr/TiO_2-Cr/Al_2O_3 diagram. The data newly acquired in this study also plot in the same area (Fig. 4). The uncertainties in Cr behavior during alteration do not require revision of this conclusion, as on this diagram the discrimination of mafic and ultramafic rocks from more felsic rocks depends largely on Zr/TiO_2 ratio that is conservative during alteration as discussed above. In Table 4, the average values and ranges of Th/Sc, Cr/Th and Cr/Zr ratios of the samples analyzed here and representative values for Archean igneous rocks (Condie and Wronkiewicz, 1990; Condie, 1993) are shown together. A Cr-free indicator, the Th/Sc ratio, is lower than 0.05 in most samples (Table 1), close to the basaltic value (0.02). Though not so sensitive as Th/Sc, the Al_2O_3/TiO_2 values also could be used as an indicator of the original rock type (e.g., Sugitani *et al.*, 1996). Archean data compiled by Sugitani (2000) show that while some mafic to ultramafic rocks have Al_2O_3/TiO_2 values lower than 10, intermediate and felsic rocks always have Al_2O_3/TiO_2 values higher than 10. The Al_2O_3/TiO_2 values of the Mt. Goldsworthy rocks are commonly lower than 10 (Table 1). These lines of evidence convincingly suggest an original mafic to ultramafic composition of the basal rocks and furthermore suggest that Cr can be regarded basically as immobile like Zr, because values of indicators using Cr content such as Cr/Th and Cr/Zr are consistent with those of other Cr-free indicators such as Th/Sc, Zr/TiO_2 and Al_2O_3/TiO_2 (Tables 1 and 4). It is inferred from these facts that Cr-redistribution during alteration was not significant. Chromium incorporated in primary minerals such as pyroxene and Cr-spinel appears to have been released during decomposition of host minerals and then re-incorporated into secondary minerals such as fuchsite and other alumino-silicates (Table 2), probably at the scale of a hand-specimen.

It may be additionally noted that there are no observed systematic differences in geochemistry between the samples showing different petrographic features. The samples without igneous textures have Zr/TiO_2 and Th/Sc values of 72.6 to 100 and 0.024 to 0.1, respectively, which cannot be discriminated from the values of the igneous-textured samples (75–104 for Zr/TiO_2 and 0.029–0.076 for Th/Sc) (Table 1). Some of these samples occasionally have clastic textures as described in the former section, implying that they represent a volcaniclastic portion. The rest of the samples without either clastic or magmatic textures may have originated from fine ash of the same composition.

Correlation with Pilbara volcanic formations and assumed original rock type

Based on the assumption that the Mt. Goldsworthy basal rocks were originally mafic to ultramafic rocks, we compare them here with Archean basaltic-komatiitic formations in the Pilbara Craton. The Pilbara basaltic-komatiitic formations comprise tholeiitic basalt (THB), tholeiitic gabbro (THG), peridotitic komatiite (PK), high-magnesian basalt (HMB) and high-alumina basalt (HAB), which can be discriminated on a Zr/TiO_2-Cr/Al_2O_3 diagram (Fig. 5). Though partially overlapping with each other, high-MgO rocks such as HMB and PK tend to have higher values of Cr/Al_2O_3 than the other types (THB, THG, and HAB). In this diagram, all of the Mt. Goldsworthy samples as well as Mt. Grant least altered samples plot within the high-MgO field, irrespective of random sampling and various lithology. It is thus unlikely that the distribution of samples in the high Cr/Al_2O_3 field resulted from Cr-redistribution and silicification. Suspected Cr-redistribution mentioned in the earlier section could be negligible in discriminating original rock type on this diagram. Consequently we infer that the heavily altered rocks were originally komatiites or high-magnesian basalts.

Though the original rock type can be assumed as discussed above, exact chemical compositions of the Mt. Goldsworthy are almost impossible to infer, due to intense alteration. High-MgO rocks in general contain >10% MgO; however MgO concentrations of the Mt. Goldsworthy rocks are mostly less than 1%, with MgO/TiO_2 values less than 1.0. Even the least altered, relatively Mg-enriched samples from Mt. Grant site have MgO concentrations less than 5%. These features are explained by removal of Mg during alteration. Additionally removal of Fe and Ca is indicated from the presence of samples with markedly low Fe_2O_3/TiO_2 (<1) and CaO/TiO_2 (<0.3). Silica-enrichment of the Mt. Goldsworthy rocks is not solely attributed to removal of these mobile elements and retention of Si. As suggested by inverse relationships of immobile elements with Si, Si has been

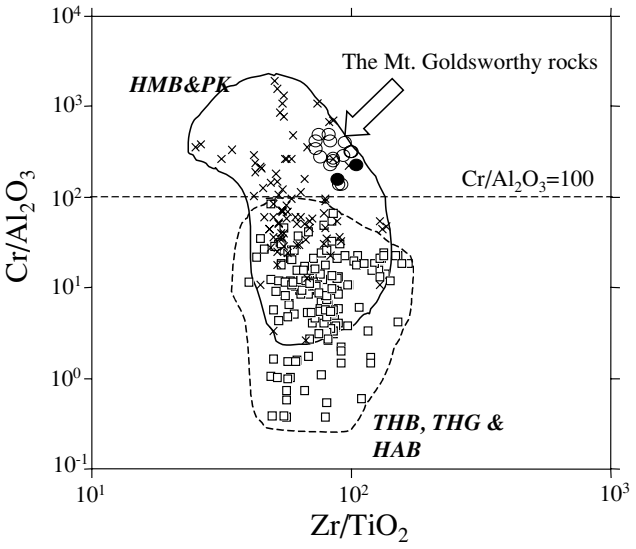

Fig. 5. Relationship between Zr/TiO_2 and Cr/Al_2O_3 for non high-MgO rocks (THB, THG and HAB) (open square) and high-MgO rocks (HMB and PK) (crosses) from Archean basaltic formations in the Warrawoona and Gorge Creek Groups in the Pilbara Block (by Budd et al., 2002; AGSO database). Open circle: sample from Mt. Goldsworthy. Closed circle: samples from Mt. Grant.

substantially added. Such intense alteration of Mt. Goldsworthy rocks makes it difficult to identify their original chemical composition. Nevertheless, the following conclusion could be made. Mt. Goldsworthy rocks are characterized by low Al_2O_3/TiO_2 values (4.6–7). The low Al_2O_3/TiO_2 values are attributed mainly to an original low concentration of Al_2O_3; even the least altered samples with SiO_2 around 65% contain less than 9% Al_2O_3. Therefore the Mt. Goldsworthy rocks may have been originally Al-depleted, in addition to MgO-enriched.

Igneous petrogenesis with implications of REE behavior

Green *et al.* (2000) suggested that the parental magma of the mafic-ultramafic volcanic rocks in the Warrawoona Group had been contaminated with crustal material (up to 25%). Such a crustal contamination model is motivated by the fact that significant depletion in mantle-derived elements such as Nb is associated with increased crustal components such as Th, LREE, and U (Arndt and Jenner, 1986; Cattel, 1987; Cattel and Arndt, 1987; Jochum *et al.*, 1991; Sun *et al.*, 1989; Rudnick and Fountain, 1995). This crustal contamination model for the Warrawoona rocks may explain the observed significant variations in trace element ratios such as La/Yb, La/Sm and Th/Sc of the Mt. Goldsworthy rocks (Fig. 3 and Table 4).

In order to test this model, we introduce here La-Sm-Yb-Th-Sc systematics, where the Th/Sc ratio is used as

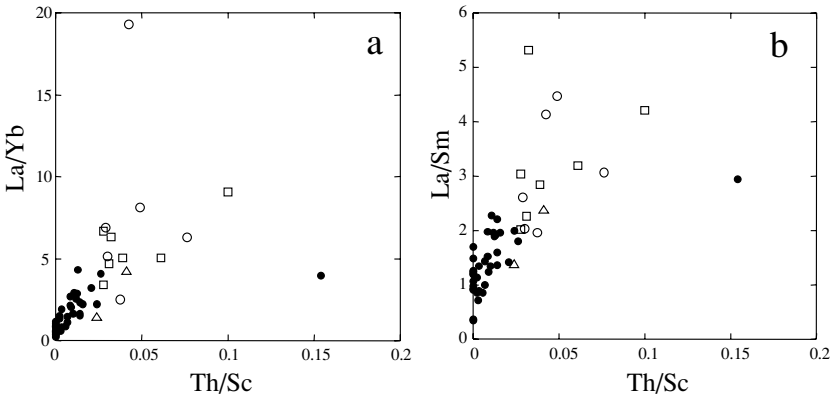

Fig. 6. Relationships between Th/Sc and La/Yb (a) and Th/Sc and La/Sm (b). Open symbols are the present data (open circle: igneous texture, open triangle: clastic texture, open square: unclear; also see Table 1). Closed circles are Warrawoona high MgO-rocks (unpublished data provided through the courtesy of Dr. Smithies, H., Geological Survey of Western Australia).

an indicator for crustal contamination, based on the Archean upper crust (Th = 5.7 ppm, Sc = 14 ppm) having a Th/Sc ratio (0.41) distinct from primitive mantle (Th = 0.064 ppm, Sc = 13 ppm) (Th/Sc = 0.005) (Taylor and McLennan, 1985) and komatiite (Th = 0.3 ppm, Sc = 28 ppm) (Th/Sc = 0.01) (Condie, 1993). In both Th/Sc-La/Yb and Th/Sc-La/Sm plots, the Mt. Goldsworthy rocks roughly define positive trends, consistent with the trend for high MgO rocks in the Warrawoona Group (unpublished data) (Fig. 6). Consequently, the observed La/Yb and La/Sm variations may be simply interpreted by crustal contamination, assuming the Th/Sc ratio, sensitive to crustal contamination, is conservative during alteration. However, the results of mixing calculations using komatiite data as an end-member for parental high-MgO magma evoke caution (Fig. 7), because half of the Mt. Goldsworthy rocks are inconsistent with any of the mixing lines using three different felsic end-members; Archean Upper Crust, TTG (tonalite-trondhjemite-granodiorite) and granite. This feature can be explained by La-redistribution during alteration and resultant perturbation of La/Yb ratio, because correlation coefficients between Th, Sc and Yb (r = 0.76 for Th-Sc and r = 7.0 for Th-Yb) are significantly higher than those between Th, La and Yb (r = 0.40 for La-Yb and r = 0.38 for La-Th) (Table 3). Several authors also reported that during alteration of Archean greenstones, the LREE contents have often been modified, whereas the HREE compositions are less affected (Arndt *et al*., 1989; Condie *et al*., 1977; Tourpin *et al*., 1991; Polat and Hofmann, 2003; Hayashi *et al*., 2004). Due to the modification of La/Yb ratios documented above, it is equivocal which line in Fig. 7 is the most likely for the mixing trend; however some samples of the Mt. Goldsworthy appear to be significantly contaminated (>10%) with crustal materials of felsic composition.

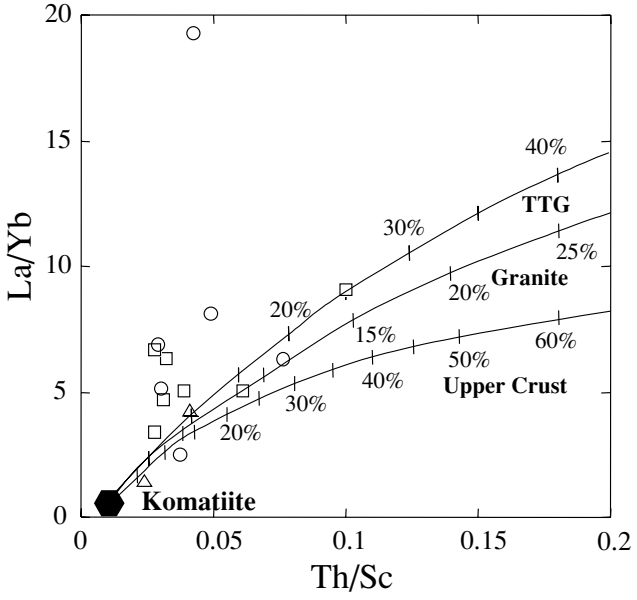

Fig. 7. Model for mixing of komatiitic magma with felsic contaminants represented by TTG, granite and the upper crustal composition, in the Th/Sc-La/Yb system. Data of TTG, granite and komatiite are from Condie (1993), whereas that of the Archean Upper Crust is from Taylor and McLennan (1985). Symbols for the Mt. Goldsworthy rocks are referred to Fig. 6.

Implications for alteration processes

As previously mentioned, the Mt. Goldsworthy rocks had been subjected to multiple alteration events; in addition to silicification, other alteration events related to the formation of carbonate (carbonatization), chlorite (chloritization) and fuchsite (K-metasomatism) are inferred. The previous presence of carbonate minerals is

indicated by the presence of rhombs composed of Fe-oxides (Fig. 2d) and of minute carbonate particles in silicified crystal pseudomorphs. The Fe-oxide rhombs are likely to have formed by oxidation of iron-rich carbonates such as ankerite and siderite, neither of which are common as primary igneous minerals but can be observed in altered volcanic rocks (Pohl *et al*., 1986; Morton and Nebel, 1984; Kitajima *et al*., 2001; Nakamura and Kato, 2004). The presence of minute carbonate particles in pseudomorphs can be interpreted to be the result of carbonatization followed by silicification of precursory non-carbonate minerals. Chlorite is abundant only in less silicified Mt. Grant samples (Fig. 2d), which does not necessarily mean that the Mt. Goldsworthy rocks were not subjected to chlorite alteration. Considering that chlorite alteration is common in Archean greenstones, the absence of chlorite in Mt. Goldsworthy samples may be attributed to later intense silicification. Potassium data obtained in this study (Table 1) reveal that K-metasomatism has occurred heterogeneously.

Alteration of the middle to lower succession of the Warrawoona mafic to ultramafic volcanic rocks well-exposed at Marble Bar and North Pole areas were extensively studied by Kitajima *et al*. (2001), Nakamura and Kato (2004) and Van Kranendonk and Pirajno (2004). These authors concluded that seafloor hydrothermal circulation is responsible for the alteration of these Warrawoona volcanic rocks, although tectonic setting and heat source is still controversial; Kitajima *et al*. (2001) and Nakamura and Kato (2004) emphasized the mid-ocean ridge type hydrothermal circulation (mantle-source), whereas Van Kranendoank and Pirajno (2004) suggested submarine caldera setting and intruding granitoid plutons as a heat source. Alteration of the upper succession of Warrawoona volcanic rocks, to which the heavily altered rocks are assigned, has been studied for samples collected from the North Pole Dome and the neighbouring area (Van Kranendonk and Pirajno, 2004). According to the authors, the alteration is thought to post-date the deposition of the overlying Strelley Pool Chert, closely related to the eruption of the overlying Euro Basalt. In addition, the reported high K_2O signature of basalts beneath the Strelley Pool Chert was attributed possibly to weathering process during subaerial exposure (Van Kranendonk and Pirajno, 2004 and references therein).

At Mt. Goldsworthy-Mt. Grant, the Euro Basalt is only distributed locally outside the map in Fig. 1. Thus, alteration related to the Euro Basalt is unclear, although the following points can be emphasized: 1) Chert dyke swarms, well developed at North Pole area, cannot be seen. 2) The Strelley Pool Chert sediments were pervasively silicified, whereas silicification of the underlying Warrawoona volcanic and volcanic rocks may have been restricted around the uppermost portion of a few tens meters, assuming that their present distribution at outcrop reflects resistance against weathering. 3) The volcanic and volcaniclastic rocks may have been sub-aerially exposed and weathered, as inferred from local erosional contact. 4) Eruption of the volcanic rocks probably occurred at a continental setting.

Apparently, the alteration process and mechanism at Mt. Goldsworthy region are not equivalent to well-documented seafloor hydrothermal alteration of the middle to lower Warrawoona rocks. Alteration of Mt. Goldsworthy rocks may have been a result of complex process including weathering and interaction with seawater at relatively low temperature, in addition to hydrothermal alteration, although the whole picture is still unclear.

CONCLUSIONS

The basal rocks at Mt. Goldsworthy region, which are assigned to the uppermost Warrwoona Group of the Pilbara Supergroup in the eastern Pilbara Craton, are composed mostly of microcrystalline quartz, iron oxides, and secondary alumino-silicates. Although they partly display magmatic textures, their chemical compositions are quite different from those of igneous rocks; SiO_2 concentrations of most samples except two exceed 80%. The rocks have been subjected to several different alteration events such as carbonatization, chloritization, K-metasomatism and silicification. The alteration is assumed to result from weathering during subaerial exposure after eruption, circulation of hydrothermal fluids and metasomatic silicification.

Despite significant modifications of their compositions, the original rock types can be revealed using the relative ratios of Al, Ti, Zr, Th, Cr and Sc, which are conservative during alteration. Geochemical indicators such as Al_2O_3/TiO_2, Zr/TiO_2, Cr/Al_2O_3, and Cr/Th all show that the Mt. Goldsworthy rocks were originally of mafic to ultramafic composition. Comparisons with data from the Pilbara basaltic formations also suggest original high-MgO compositions (i.e., komatiite, high-MgO basalt) and possibly Al-depletion. La-Sm-Yb-Th-Sc systematics also imply crustal contamination of the parental magma, which is consistent with the assumed depositional environment of the overlying Strelley Pool Chert and the early development of the continental crust.

Acknowledgments—We wish to express our gratitude to Dr. K. Tainosho of Kobe University, who helped us with the X-ray fluorescence analyses for minor elements, and to Dr. K. Nagamine and Dr. K. Mimura of Nagoya University, and Dr. R. Sugisaki, an emeritus professor of Nagoya University for their assistance in sampling. We also would like to thank Dr. K. Kitajima, Dr. K. Shimizu and Dr. A. Polat for their helpful reviews.

References

Anders, E. and Grevesse, N. (1989) Abundances of the elements: meteoritic and solar. *Geochim. Cosmochim. Acta* **53**, 197–214.

Arndt, N. T. (1994) Archean komatiites. *Archean Crustal Evolution. Developments in Precambrian Geology 11* (Condie, K. C., ed.), 11–44, Elsevier, Amsterdam.

Arndt, N. T. and Jenner, G. A. (1986) Crustally contaminated komatiites and basalts from Kambalda, Western Australia. *Chem. Geol.* **56**, 229–255.

Arndt, N. T., Teixeira, N. A. and White, W. M. (1989) Bizarre geochemistry of komatiites from the Crixás greenstone belt, Brazil. *Contrib. Mineral. Petrol.* **101**, 187–197.

Barley, M. E. (1993) Volcanic, sedimentary and tectonostratigraphic environments of the ~3.46 Ga Warrawoona Megasequence: a review. *Precambrian Res.* **60**, 47–67.

Budd, A. R., Hazell, M., Sedgmen, A. and Sedgmen, L. (Kilgour, B., compiler) (2002) OZCHEM National Whole Rock Geochemistry Database (Digital Dataset). Geoscience Australia, Canberra.

Buick, R., Thornett, J. R., McNaughton, N. J., Smith, J. B., Barley, M. E. and Savage, M. (1995) Record of emergent continental crust ~3.5 billion years ago in the Pilbara Craton of Australia. *Nature* **375**, 574–577.

Cattell, A. (1987) Enriched komatiitic basalts from Newton Township, Ontario: their genesis by crustal contamination of depleted komatiite magma. *Geol. Mag.* **124**, 303–309.

Cattell, A. and Arndt, N. (1987) Low- and high-alumina komatiites from a Late Archean sequence, Newton Township, Ontario. *Contrib. Mineral. Petrol.* **97**, 218–227.

Condie, K. C. (ed.) (1981) Archean greenstone belts. *Developments in Precambrian Geology 3*, 67–130, Elsevier, Amsterdam.

Condie, K. C. (1993) Chemical composition and evolution of the upper continental crust: contrasting results from surface samples and shales. *Chem. Geol.* **104**, 1–37.

Condie, K. C. and Wronkiewicz, D. J. (1990) The Cr/Th ratio in Precambrian pelites from the Kaapvaal Craton as an index of cratonic evolution. *Earth Planet. Sci. Lett.* **97**, 256–267.

Condie, K. C., Viljoen, M. J. and Kable, E. J. D. (1977) Effects of alteration on element distributions in Archean tholeiites from the Barberton greenstone belt, South Africa. *Contrib. Mineral. Petrol.* **64**, 75–89.

Cullers, R. L., DiMarco, M. J., Lowe, D. R. and Stone, J. (1993) Geochemistry of a silicified, felsic volcaniclastic suite from the early Archean Panorama Formation, Pilbara Block, Western Australia: an evaluation of depositional and postdepositional processes with special emphasis on the rare-earth elements. *Precambrian Res.* **60**, 99–116.

Duchač, K. C. and Hanor, J. S. (1987) Origin and timing of the metasomatic silicification of an early Archean komatiite sequence, Barberton Mountain Land, South Africa. *Precambrian Res.* **37**, 125–146.

Enami, M., Mizukami, T. and Yokoyama, K. (2004) Metamorphic evolution of garnet-bearing ultramafic rocks from the Gongen area, Sambagawa belt, Japan. *J. Metamorphic Geol.* **22**, 1–15.

Gao, S. and Wedepohl, K. H. (1995) The negative Eu anomaly in Archean sedimentary rocks: Implications for decomposition, age and importance of their granitic sources. *Earth Planet. Sci. Lett.* **133**, 81–94.

Glikson, A. Y. and Hickman, A. H. (1981) Geochemical stratigraphy and petrogenesis of Archaean basic-ultrabasic volcanic units, eastern Pilbara Block, Western Australia. *Spec. Publs Geol. Soc. Aust.* **7**, 287–300.

Green, M. G., Sylvester, P. J. and Buick, R. (2000) Growth and recycling of early Archaean continental crust: geochemical evidence from the Coonterunah and Warrawoona Groups, Pilbara Craton, Australia. *Tectonophysics* **322**, 69–88.

Gruau, G., Tourpin, S., Fourcade, S. and Blais, S. (1992) Loss of isotopic (Nd, O) and chemical (REE) memory during metamorphism of komatiites; new evidence from eastern Finland. *Contrib. Mineral. Petrol.* **112**, 68–82.

Hayashi, T., Tanimizu, M. and Tanaka, T. (2004) Origin of negative Ce anomalies in Barberton sedimentary rocks, deduced from La-Ce and Sm-Nd isotope systematics. *Precambrian Res.* **135**, 345–357.

Hickman, A. H. (1983) Geology of the Pilbara Block and its environs. *West. Aust. Geol. Surv. Bull.*, **127**.

Jochum, K. P., Arndt, N. T. and Hofmann, A. W. (1991) Nb-Th-La in komatiites and basalts: constraints on komatiite petrogenesis and mantle evolution. *Earth Planet. Sci. Lett.* **107**, 272–289.

Kitajima, K., Maruyama, S., Utsunomiya, A. and Liou, J. G. (2001) Seafloor hydrothermal alteration at an Archaean mid-ocean ridge. *J. Metamorphic Geol.* **19**, 583–599.

Lowe, D. R. (1980) Stromatolites 3,400-Myr old from the Archean of Western Australia. *Nature* **284**, 441–443.

Lowe, D. R. (1983) Restricted shallow-water sedimentation of Early Archean stromatolitic and evaporitic strata of the Strelley Pool Chert, Pilbara Block, Western Australia. *Precambrian Res.* **19**, 239–283.

Lowe D. R. (1999) Petrology and sedimentology of cherts and related silicified sedimentary rocks in the Swaziland Supergroup. *Geol. Soc. Am. Spec. Paper* **329**, 83–114.

McCuaig, T. C., Kerrich, R. and Xie, Q. (1994) Phosphorus and high field strength element anomalies in Archean high-magnesian magmas as possible indicators of source mineralogy and depth. *Earth Planet. Sci. Lett.* **124**, 221–239.

McNaughton, N. J., Compston, W. and Barley, M. E. (1993) Constraints on the age of the Warrawoona Group, eastern Pilbara Block, Western Australia. *Precambrian Res.* **60**, 69–98.

Morton, R. L. and Nebel, M. J. (1984) Hydrothermal alteration of felsic volcanic rocks at the Helen siderite deposit. Wawa, Ontario. *Econ. Geol.* **79**, 1319–1333.

Nakamura, K. and Kato, Y. (2004) Carbonatization of oceanic crust by the seafloor hydrothermal activity and its significance as a CO_2 sink in the Early Archean. *Geochim. Cosmochim. Acta* **68**, 4595–4618.

Nisbet, E. G., Martin, A., Bickle, M. J. and Orpen, J. L. (1993) The Ngezi Group: Komatiite, basalts and stromatolites on continental crust. *The Geology of the Belingwe Greenstone Belt, Zimbabwe. Geol. Soc. Zimbabwe Special Publication 2* (Bickle, M. J. and Nisbet, E. G., eds.), 121–165.

Orpen, J. L., Martin, A., Bickle, M. J. and Nisbet, E. G. (1993) The Mtshingwe Group in the west: Andesite, basalts,

komatiites and sediments of the Hokonui, Bend and Koodoovale Formations. *The Geology of the Belingwe Greenstone Belt, Zimbabwe*. *Geol. Soc. Zimbabwe Special Publication 2* (Bickle, M. J. and Nisbet, E. G., eds.), 69–86.

Pohl, W., Anouri, M., Kolli, O., Scheffer, R. and Zachmann, D. (1986) A new genetic model for the North African metasomatic siderite deposits. *Mineral. Deposita* **21**, 228–233.

Polat, A. and Hofmann, A. W. (2003) Alteration and geochemical patterns in the 3.7–3.8 Ga Isua greenstone belt, West Greenland. *Precambrian Res.* **126**, 197–218.

Polat, A., Kerrich, R. and Wyman, D. A. (1999) Geochemical diversity in oceanic komatiites and basalts from the late Archean Wawa greenstone belts, Superior Province, Canada: trace element and Nd isotope evidence for a heterogeneous mantle. *Precambrian Res.* **94**, 139–173.

Polat, A., Hofmann, A. W. and Rosing, M. T. (2002) Boninite-like volcanic rocks in the 3.7–3.8 Ga Isua greenstone belt, West Greenland: geochemical evidence for intra-oceanic subduction zone processes in the early Earth. *Chem. Geol.* **184**, 231–254.

Rudnick, R. L. and Fountain, D. M. (1995) Nature and composition of the continental crust: a lower mantle perspective. *Rev. Geophys.* **33**, 267–309.

Salvi, S. and Williams-Jones, A. E. (1996) The role of hydrothermal processes in concentrating high-field strength elements in the Strange Lake peralkaline complex, northeastern Canada. *Geochim. Cosmochim. Acta* **60**, 1917–1932.

Shibata, S., Tanaka, T., Minami, M., Senda, R., Takebe, M., Kachi, T., Kondo, M., Oda, S., Hayashi, T., Nishizawa, K. and Kojima, H. (2001) The procedure and accuracy of INAA for geological materials by new γ-ray counting and data processing system at Radioisotope Center in Nagoya University. *Bull. Nagoya Univ. Museum* **17**, 15–32.

Smith, H. S., Erlank, A. J. and Duncan, A. R. (1980) Geochemistry of some ultramafic komatiite lava flows from the Barberton Mountain Land, South Africa. *Precambrian Res.* **11**, 399–415.

Smith, H. S., O'Neil, J. R. and Erlank, A. J. (1984) Oxygen isotope compositions of minerals and rocks and chemical alteration patterns in pillow lavas from the Barberton Greenstone Belt, South Africa. *Archean Geochemistry (The Origin and Evolution of the Archean Continental Crust)* (Kröner, A. *et al*., eds.), 115–137, Springer-Verlag, Berlin.

Smithies, R. H. (2002) De Grey, W.A. Sheet 2757: Western Australia Geological Survey, 1:100,000 Geological Series.

Smithies, R. H., Van Kranendonk, M. J. and Champion, D. C. (2005) It started with a plume—early Archaean basaltic proto-continental crust. *Earth Planet. Sci. Lett.* **238**, 284–297.

Smithies, R. H., Hickman, A. H. and Nelson, D. R. (1999) New constraints on the evolution of the Mallina Basin, and their bearing on relationships between the contrasting eastern and western granite-greenstone terranes of Archaean Pilbara Craton, Western Australia. *Precambrian Res.* **94**, 11–28.

Smithies, R. H., Champion, D. C. and Cassidy, K. F. (2003) Formation of Earth's early Archaean continental crust. *Precambrian Res.*, **127**, 89–101.

Sugisaki, R., Shimomura, T. and Ando, K. (1977) An automatic X-ray fluorescence method for the analysis of silicate rocks. *Jour. Geol. Soc. Jpn.* **83**, 725–733 (in Japanese).

Sugitani, K. (2000) Al-Ti-Cr-Zr systematics of Archean igneous rocks and its application to metasomatically-silicified igneous rocks and provenance analyses of sedimentary rocks. *Stud. Inform. Sci. Nagoya Univ.* **12**, 1–17 (in Japanese).

Sugitani, K. and Mimura, K. (1998) Redox change in sedimentary environments of Triassic bedded cherts, central Japan: possible reflection of sea-level change. *Geol. Mag.* **135**, 735–753.

Sugitani, K., Horiuchi, Y., Adachi, M. and Sugisaki, R. (1996) Anomalously low Al_2O_3/TiO_2 values for Archean cherts from the Pilbara Block, Western Australia-possible evidence for extensive chemical weathering on the early earth. *Precambrian Res.* **80**, 49–76.

Sugitani, K., Mimura, K., Suzuki, K., Nagamine, K. and Sugisaki, R. (2003) Stratigraphy and sedimentary petrology of an Archean volcanic-sedimentary succession at Mt. Goldsworthy in the Pilbara Block, Western Australia: implications of evaporite (nahcolite) and barite deposition. *Precambrian Res.* **120**, 55–79.

Sun, S.-S. and Nesbitt, R. W. (1978) Petrogenesis of Archaean ultrabasic and basic volcanics: Evidence from rare earth elements. *Contrib. Mineral. Petrol.* **65**, 301–325.

Sun, S.-S., Nesbitt, R. W. and McCulloch, M. T. (1989) Geochemistry and petrogenesis of Archaean and early Proterozoic siliceous high-magnesian basalts. *Boninites* (Crawford, A. J., ed.) 148–173, Unwin Hyman, London.

Taylor, S. R. and McLennan, S. M. (1985) *The Continental Crust: Its Composition and Evolution*. Blackwell Scientific Publications, Oxford.

Thorpe, R. I., Hickman, A. H., Davis, D. W., Mortensen, J. K. and Trendall, A. F. (1992) U-Pb zircon geochronology of Archaean felsic units in the Marble Bar region, Pilbara Craton, Western Australia. *Precambrian Res.* **56**, 169–189.

Tourpin, S., Gruau, G., Blais, S. and Fourcade, S. (1991) Resetting of REE, and Nd and Sr isotopes during carbonitization of a komatiite flow from Finland. *Chem. Geol.* **90**, 15–29.

Van Kranendonk, M. J. and Pirajno, F. (2004) Geochemistry of metabasalts and hydrothermal alteration zones associated with *c*. 3.45 Ga chert and barite deposits: implications for the geological setting of the Warrwoona Group, Pilbara Craton, Australia. *Explor. Environ. Anal.* **4**, 253–278.

Van Kranendonk, M. J., Hickman, A. H., Smithies, R. H. and Nelson, D. R. (2002) Geology and tectonic evolution of the Archean North Pilbara Terrain, Pilbara Craton, Western Australia. *Econ. Geol.* **97**, 695–732.

Van Kranendonk, M. J., Smithies, H., Hickman, A. H., Bagas, L., Williams, I. R. and Farrell, T. R. (2004) Event stratigraphy applied to 700 million years of Archaean crustal evolution, Pilbara Craton, Western Australia. *Annual Review2003–4, Geological Survey of Western Australia*, 49–61.

Xie, Q., Kerrich, R. and Fan, J. (1993) HFSE/REE fractionations recorded in three komatiite-basalt sequences, Archean Abitibi greenstone belt: Implications for multiple plume sources and depths. *Geochim. Cosmochim. Acta* **57**, 4111–4118.